Thermochimica Acta, 161 (1990) 37–49
Elsevier Science Publishers B.V., Amsterdam – Printed in The Netherlands

USING THERMOANALYTICAL DATA. PART 2. THE DEPENDENCE OF KINETIC DATA AVAILABLE FROM THERMOGRAVIMETRY ON SAMPLE AND INSTRUMENT PARAMETERS: A METHOD FOR CALCULATING 'TRUE' KINETIC PARAMETERS

U. BIADER CEIPIDOR

Istituto di Chimica, Universitá della Basilicata, Via N. Sauro, 85100 Potenza (Italy)

R. BUCCI * and A.D. MAGRÍ

Dipartimento di Chimica, Universitá La Sapienza, P. le A. Moro, 00185 Roma (Italy)

(Received 9 August 1989)

ABSTRACT

Kinetic data available from TG measurements are discussed with respect to thermal coefficients such as sample specific heat, reaction enthalpy, instrument heat-transfer coefficient and heat capacity. The dependence of the available kinetic parameters Z, E and N on these thermal coefficients is examined using a numerical model. A relationship is also derived for calculating the kinetic parameters from experimental TG curves whilst taking into account the perturbation induced by the above-cited thermal coefficients. The dehydration of calcium oxalate is used to evaluate experimentally the predictive power of the kinetic parameters obtained in this way, i.e. their ability to describe the sample behaviour under a wide range of operational conditions (different masses and heating rates), including isothermal reactions.

INTRODUCTION

Whilst TG measurements were originally used for analytical purposes, based on mass ratios between thermal decomposition products and reagents instrumental techniques have evolved to allow the study of reaction kinetics. Finding a way to predict the behaviour of materials under extreme heating conditions [1,2], as well as to determine kinetic parameters to be used for chemical characterization [3], is of increasing interest.

In a previous work [4] the limitations of describing the varying behaviour of materials using TG measurements of the kinetic parameters Z, E and N, appearing in an empirical differential equation derived from the Arrhenius kinetic law, were discussed. The ability of an obtained (Z, E, N) triplet to

* Author to whom correspondence should be addressed.

0040-6031/90/$03.50 © 1990 Elsevier Science Publishers B.V.

describe a more general sample behaviour under heating, which we called the predictive power, should in fact be increased when heat transfer (taking place during the experiment) is included in the calculation.

Several mathematical manipulations have been proposed to improve (Z, E, N) calculations [5–8] and to fit TG data to more sophisticated kinetic laws [9–12] or to consecutive reactions [13], always without taking into account the instrument thermal geometry and consequently the heat transfer effect on measured parameters. At the point where the sample mass and heating rate are sufficiently low this influence may be reduced. This condition however, only occurs infrequently, thus explaining the failure of many literature data to represent experimental behaviour [4]. The need to check the obtained parameters with respect to their power to reconstruct experimental data has already been highlighted [13,14].

The aim of this work is to provide a method for calculating the (Z, E, N) triplet for a given thermal reaction step with no (or limited) influence of the instrument characteristics and sample thermal properties. To check the results, simultaneous differential equation processing was first implemented, in a way suitable for PCs to reconstruct TG curves from kinetic parameters, also taking into account instrument and sample thermal coefficients. The contribution of the same thermal coefficients was then introduced into the previously proposed differential approach [4] to the calculation of kinetic parameters from TG curves.

By comparing the reconstructed TG curves with the experimental ones and by comparing calculated and measured isothermal half-lives, the predictive power of the kinetic parameters obtained in this way was discussed. The dehydration of calcium oxalate [15] was used as a test.

EXPERIMENTAL

Thermogravimetric measurements were carried out using a Perkin–Elmer TGS-2 instrument, operating under a dynamic nitrogen atmosphere flowing at 50 ml min^{-1}. Both isothermal and programmed heating runs were performed. Calorimetric determinations were made on a Mettler TA3000 DSC system using the same nitrogen flow; indium was used for calibration. Calculations were implemented on an IBM-compatible PC, operating in MS-DOS 3.25, using an MS-GWBASIC 3.25 interpreter and an MS-BASIC 2.00 compiler.

Model and symbols

When a solid sample S is heated it may react as follows

$$S \rightarrow P + G \qquad (1)$$

where P is the solid product and G the evolved gas. The kinetics of this reaction, already reported in a complete form taking into account solid nucleation and growth, phase boundary process and diffusion through the sample [16], are generally postulated to follow a more simple Arrhenius-type equation. Reasonable assumptions are that the process of solid thermal decomposition is mainly governed by phase boundary reactions and that the contribution of the other mechanisms may be described by an apparent order of reaction which is different from the theoretical one (i.e. $\frac{2}{3}$ for a three-dimensional sample)

$$-(\mathrm{d}W/\mathrm{d}t) = Z \exp(-E/(RT))W^N \tag{2}$$

where W is the fraction of reagents (or 1 − W is the extent of reaction), t is the time (in s), T is the absolute temperature (in K), R is the gas constant (in J K^{-1} per apparent g mole), Z is the pre-exponential factor (in s^{-1}), E is the activation energy (in J per apparent g mole) and N is the apparent order of reaction. The above representation does not take into account the influence of the pressure of the evolved gas, formally introducing a dependence of E on T, t and mainly on gas type and transport outside the sample holder. The use of an external gas flow and a small sample holder drastically reduces this dependence except when sealed tubes are used [17].

A common way to evaluate W in eqn. (2) has been previously described together with its physical meaning) [4]

$$W = (m - m_f)/(m_i - m_f) \tag{3}$$

where m is the actual mass (at a given time), m_i is the initial mass and m_f is the final mass. When considering the thermal geometry of a TG apparatus, the heat transfer between the heater and the sample could be modelled as described below. This is a way to assign an explicit form to the F11, F21–F23 functions previously reported [4].

As a first approximation the heat flow from the heater to the sample holder follows the general rule of force-driven flows,

$$Q1 = k(T_p - T) \tag{4}$$

where k is an overall transfer coefficient, T_p is the programmed temperature of the heater and T is the sample temperature (assumed to be the same as that of the holder). This heat flow, however, should balance the rate of temperature variation in both holder and sample and, if a reaction occurs, the rate of absorbed thermal energy Q_r,

$$Q2 = C_{t0}(\mathrm{d}T/\mathrm{d}t) + C_{so}m(\mathrm{d}T/\mathrm{d}t) + \mathrm{d}Q_r/\mathrm{d}t \tag{5}$$

where C_{t0} is the sample holder heat capacity, C_{so} is the actual sample specific heat and m is the actual reacting sample mass. The sample heat capacity $C_{so}m$ is that of a mixture of reactant S and product P. If taking into

account the specific heats and masses of S and P (C_s, M_s and C_p M_p respectively), it can be rewritten as

$$C_{so}m = C_sM_s + C_pM_p \qquad \text{or} \qquad C_{so}m = \left(C_sM_s/m_i + C_pM_p/m_im_i\right) \tag{6}$$

It was pointed out [4] that $W = M_s/m_i$ and $1 - W = M_p/m_f$, giving

$$C_{so}m = \left(C_sW + C_p(m_f/m_i)(1 - W)\right)m_i \tag{7}$$

By defining $C1 = C_s$, specific heat of reactant, and $C2 = C_p(m_f/m_i)$, specific heat of product referred to the mass of the reactant, the following often-assumed expression can be derived

$$C_sm = \left(C1W + C2(1 - W)\right)m_i \tag{8}$$

By treating the absorbed reaction heat as the energy per unit mass of reactant (when considering a temperature-independent reaction enthalpy H), the following expression can be obtained

$$\mathrm{d}Q_r/\mathrm{d}t = -m_iH\,\mathrm{d}W/\mathrm{d}t \tag{9}$$

The above two relationships, combined with the $Q2$ expression, allow the energy balance to be written in a usable form implying that the heat flow $Q1$ be equal to $Q2$, i.e.:

$$k\left(T_p - T\right) = \left\{C_{t0} + m_i\left[C1W + C2(1 - W)\right]\right\}(\mathrm{d}T/\mathrm{d}t) - m_iH(\mathrm{d}W/\mathrm{d}t) \tag{10}$$

The coefficients have the following units: k, mcal °C s^{-1}; C_{t0}, mcal °C^{-1}; $C1$, cal °C^{-1} g^{-1}; $C2$, cal °C^{-1} g^{-1}; H, cal g^{-1}; m_i, mg; T_p and T, °C, and t, s.

Using the assumption that k, C_{t0}, $C1$, $C2$ and H do not vary much during the reaction, equations (2) and (10), combined with the constant controlled heating rate $B_p = \mathrm{d}T_p/\mathrm{d}t$, describe a system of differential equations which can be solved using the following boundary conditions before the start of the reaction

$$\left.\begin{aligned} &\mathrm{d}T/\mathrm{d}t = \mathrm{d}T_p/\mathrm{d}t = B_p \\ &T = T_p - (C_{t0} + m_iC1)B/k \\ &W = 1 \\ &\mathrm{d}W/\mathrm{d}t = 0 \end{aligned}\right\} \tag{11}$$

The conditions describe the steady state of a sample heated at rate B_p with no reactions occurring.

The way the system resolution has been implemented is based on finite element analysis, i.e. on the incremental calculation of W and T, at a given $T_p = T_{po} + \mathrm{d}T_p$ (or $t = t_o + \mathrm{d}T_p/B_p$) step, from W_o, T_o, $\mathrm{d}W_o$ and $\mathrm{d}T_o$ of the

previous step. The first 'previous' step is described by the above-defined boundary conditions. From eqn. (2) it follows that

$$\begin{aligned} dW &= -Z \exp[-E/(RT_0)](W_0^N)\, dt \\ W &= W_0 + dW \end{aligned} \tag{12}$$

from differentiation of eqn. (10) with respect to T, T_p, W, dW/dt and dT/dt

$$\begin{aligned} dT &= G1/G2 \\ T &= T_0 + dT \end{aligned} \tag{13}$$

where the coefficients $G1$ and $G2$ are

$$G1 = dT_p + m_i(a1 + a2W)(dT_0/dt) + m_i a3(dW - dW_0)/dt \tag{14}$$

$$G2 = 1 + m_i[a1 + a2(W + dW)](1/dt) \tag{15}$$

and $a1$, $a2$ and $a3$ are mixed thermal coefficients, depending on the sample and equipment. They are defined as $a1 = (C_{t0}/m_i + C2)/k$, $a2 = (C1 - C2)/k$ and $a3 = H/k$.

The whole range is scanned in assigned dT_p (or $dt = dT_p/B_p$) steps, performing the above-described calculations. Each step is divided by two, four, eight, and so on into substeps, and calculations are repeated until a convergence to the final values of W and dT/dt for the processed step is achieved. The convergence is checked through absolute differences between actual W and dT/dt values at the end of the step and the same values calculated using half the number of substeps (previous iteration). They must result in tolerances which are lower than those assumed. Tolerance values used were $0.01/N_{Tot}$ and $0.01B_p$ for W and dT/dt respectively, where N_{Tot} is the total number of steps chosen to describe the entire reaction range.

The first T_p value, corresponding to the lower one in the chosen range, is checked for a calculated $dW > -0.01/N_{Tot}$ before accepting it as the boundary value. If the condition is not true, the thermal decomposition is assumed to begin at a lower temperature and a new starting T_p value, satisfying the condition, is found by lowering the T_p in steps corresponding to the whole range. When the right T_p is found, calculations are performed up to the initial temperature of the chosen range and the W, T, dT/dt and dW/dt values obtained are used as the new boundary conditions. In such a way, correct simulated TG curves can be obtained also when crossing the chosen starting temperature with W values of less than 1.

To enhance the speed of computing, the initial number of substeps (into which the next step has to be divided) is either taken to be equal to that used for the previous step (to match tolerance conditions) or to half this number, depending on whether the number of substeps required increases when passing from one step to the next. The calculations thus generally start with two substeps, required when W is close to unity, and become more accurate

using an increasing number of substeps when $0 < W < 1$, and return to the use of just two steps when W approaches zero.

By this method, simulations were performed to calculate W vs. T_p curves, as experimentally obtained, as well as W vs. T and dT/dt vs. T curves, which are experimentally unavailable, by varying m_i, B_p, $C1$, $C2$, H, $Ct0$ and k and Z, E and N.

Provided that the set of (W, T_p) couples gives values which are sufficiently close to allow numerical differentiation (i.e. $dW/dT_p = DW/DT_p$), a method for determining Z, E and N from TG curves has been previously reported using a logarithmic representation of eqn. (2) [4]

$$\log(-DW/DT) + \log(B) = \log(Z) - e/T + N \log(W) \tag{16}$$

where $e = E/(2.3R)$ is the reduced activation energy.

When the assumption needed to use this relationship for calculating kinetic parameters (i.e. $T = T_p$ and $B = dT/dt = B_p$) is not realistic, the same relationship must be combined with eqn. (10). Equation (10) can be rewritten using the above-defined mixed thermal coefficients, eqns. (14) and (15), and taking into account that $dW/dt = (dW/dT_p)(dT_p/dt)$

$$T_p - T = a1m_i B + a2m_i BW - a3m_i B_p(dW/dT_p) \tag{17}$$

and the terms of eqn. (16) containing T can be expressed as functions of the experimentally observed T_p

$$\log(-DW/DT) = \log\left[(-DW/DT_p)(DT_p/Dt)(Dt/DT)\right]$$
$$= \log\left[(-DW/DT_p)B_p/B\right] \tag{18}$$

$$e/T = e/\left[T_p - (T_p - T)\right] \approx (e/T_p)\left[1 + (T_p - T)/T_p\right] \tag{19}$$

By combining eqn. (17) with the above relationships, eqn. (16) becomes

$$\log(-DW/DT_p) + \log(B_p)$$
$$= \log(Z) - e/T_p + N \log(W) - a1m_i e\left(B/T_p^2\right) - a2m_i e\left(BW/T_p^2\right)$$
$$+ a3m_i e\left(B_p/T_p^2\right)(DW/DT_p) \tag{20}$$

Owing to the presence of the sample heating rate B, eqn. (20) should be used together with eqn. (17) to calculate kinetic parameters as well as mixed thermal coefficients from the experimentally observed W–T_p couples at given m_i and B_p values, i.e. from TG curves. The iterative procedure is summarized in (i)-(vi) below.

(i) Choose a T_p range where $0.01 < W < 0.99$ and smooth the TG curves to reduce noise perturbation on finite derivatives calculation; set the T_p data vector, where each element is taken by dividing the whole temperature range into steps, short enough to allow finite derivatives to be calculated on the corresponding values of the W data vector.

(ii) Fill a guest T vector with values corresponding to the T_p ones.

(iii) Calculate B values, corresponding to each T_p, by finite differentiation, i.e. $B = DT/Dt = (DT/DT_p)B_p$ (the use of a parabolic interpolation on T–T_p couples contributes to smooth the obtained derivatives).

(iv) Use a multi-variable linear regression to calculate Z, e, N, $ea1$, $ea2$ and $ea3$ from eqn. (20): $\log(-DW/DT_p) + \log(B_p)$ vs. $1/T_p$, $\log(W)$, $m_i B/T_p^2$, $m_i BW/T_p^2$, $m_1 B_p(1/T_p^2)(DW/DT_p)$.

(v) Use the $a1$, $a2$ and $a3$ values found, together with m_i, B_p and W–T_p couples, to calculate new T values corresponding to each T_p, using eqn. (13).

(vi) Repeat the process from step (iii) until convergence of Z, E, N, $a1$, $a2$ and $a3$ values.

Using this procedure kinetic parameters and mixed thermal coefficients can be calculated from a single TG curve as well as by simultaneous processing of many TG curves at different B_p values for given m_i values.

The parameters and coefficients obtained allow reconstruction of the calculated TG curves as described above, i.e. by combination of eqns. (2) and (17) in the finite elements analysis, in order to evaluate the agreement with the experimental curves.

Finally, half-life times may be calculated and compared with those experimentally observed during isothermal reactions. By integrating eqn. (2) when N is different from unity,

$$t_{\frac{1}{2}} = (1/Z)\exp[E/(RT)](1 - 0.5^{1-N})/(1 - N) \tag{21}$$

or, when $N = 1$,

$$t_{\frac{1}{2}} = -(1/Z)\exp[E/(RT)]\ \ln 0.5 \tag{22}$$

RESULTS

The sample reaction investigated is

$$CaC_2O_4 \cdot H_2O \rightarrow CaC_2O_4 + H_2O\uparrow \tag{23}$$

For this reaction the TG curves were recorded at several masses and heating rates. Apparent kinetic parameters were determined for each curve using the previously reported method [4], i.e. by linear regression of eqn. (16) when considering $T = T_p$ and $B = B_p$. While the kinetic parameters determined in this way display a low predictive power (each Z, E, N triplet differs considerably from the others), they allow reconstruction of calculated TG curves which match closely the experimental ones from which each triplet has been derived [4]. The reconstruction procedure in this case is the same as the above-proposed finite elements analysis using eqns. (2) and (17) taking $a1 = a2 = a3 = 0$. The results obtained are listed in Table 1.

TABLE 1

Calcium oxalate dehydration. Kinetic parameters obtained by applying the differential method [4] to each experimental TG curve

Mass (mg)	Heating rate (°C min^{-1})	Z (s^{-1})	E (kJ mol^{-1})	N
10	2.5	1.843×10^{12}	117.4	0.597
10	10	8.514×10^{7}	84.9	0.514
10	20	1.172×10^{6}	70.0	0.530
10	40	5.404×10^{5}	67.6	0.637
20	2.5	1.019×10^{7}	79.2	0.365
20	10	5.700×10^{5}	69.5	0.456
20	20	4.054×10^{4}	59.5	0.500
20	40	1.907×10^{4}	57.3	0.616

The TG curves calculated in this way were used as 'smoothed experimental' curves to calculate 'true' kinetic parameters as well as mixed thermal coefficients, using the above-described iterative procedure. Owing to the low numerical stability of a linear regression over five variables (see eqn. (20)), the $a2$ coefficient was assumed to be zero, thus reducing the number of variables to four. By applying the iterative procedure simultaneously to all the smoothed experimental curves, represented by the parameters listed in Table 1, the following values were obtained: $Z = 1.870 \times 10^{8}$ s^{-1}; $E = 86.5$ kJ mol^{-1}; $N = 0.619$; $a1 = 0.79$ s mg^{-1}; and $a3 = 234$ s °C mg^{-1}. Five iterations were needed to converge. Even though the mixed thermal coefficient $a1$ includes the sample mass (see definition), the values obtained were nearly independent of the mass itself, i.e. the differences between values obtained by processing TG curves at different mass values were not significant. The best results were thus obtained by processing the entire set of curves, as reported above.

Using DSC measurements, the enthalpy H of the investigated reaction was determined, as well as the specific heat C_p of the reaction product (anhydrous calcium oxalate) around 100 °C: $H = 86$ cal g^{-1} and $C_p = 0.28$ cal $°C^{-1}$ g^{-1}. The specific heat of the reagent C_s cannot be measured at around the temperature of reaction owing to the beginning of dehydration; an estimate obtained by extrapolating values up to 50 °C accounts for 0.28–0.29 cal $°C^{-1}$ g^{-1}.

Figures 1A and 1B show the TG curves calculated by applying finite elements analysis to the model described by the Z, E, N, $a1$ and $a3$ values, together with the corresponding smoothed experimental curves. In Table 2 the temperature differences between the experimental and calculated curves are summarized at 25%, 50% and 75% of reaction, i.e. at $W = 0.75$, $W = 0.50$ and $W = 0.25$, to evaluate the agreement numerically. To show how the reconstruction procedure works, some examples using experimental and

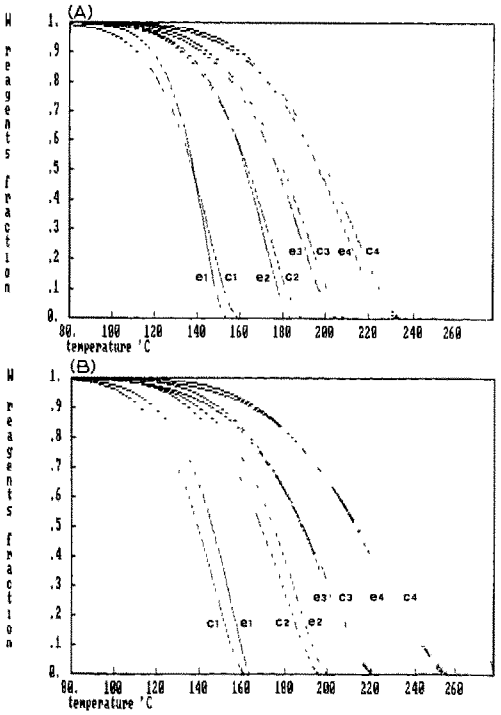

Fig. 1. Calcium oxalate dehydration. Calculated (c) and smoothed experimental (e) TG curves of W vs. T_p. W is $(m - m_f)/(m_i - m_f)$ and T_p is the heater temperature in °C. A, $m_i = 10$ mg; B, $m_i = 20$ mg. Heating rates in °C min^{-1} are: (1) 2.5; (2) 10; (3) 20; (4) 40.

simulated parameters are reported in Figs. 2A–2D. The values of C_{t0}, k, $C1$, $C2$ and H, displayed in Figs. 2A and 2B, were calculated from the mixed thermal coefficients obtained ($C1 = C2$ was assumed to match $A2 = 0$) and from the measured H and C_p for a self-explaining picture, while $a1$, $a2$ and

TABLE 2

Calcium oxalate dehydration. Temperature differences (in °C) at several extents of reaction between smoothed experimental and calculated TG curves

Mass (mg)	Heating rate (°C min^{-1})	25% reaction	50% reaction	75% reaction
10	2.5	3	0	−2
10	10	1	−1	−3
10	20	−2	−2	−3
10	40	−2	−3	−4
20	2.5	6	5	5
20	10	6	5	4
20	20	−1	−1	−1
20	40	−1	−2	−2

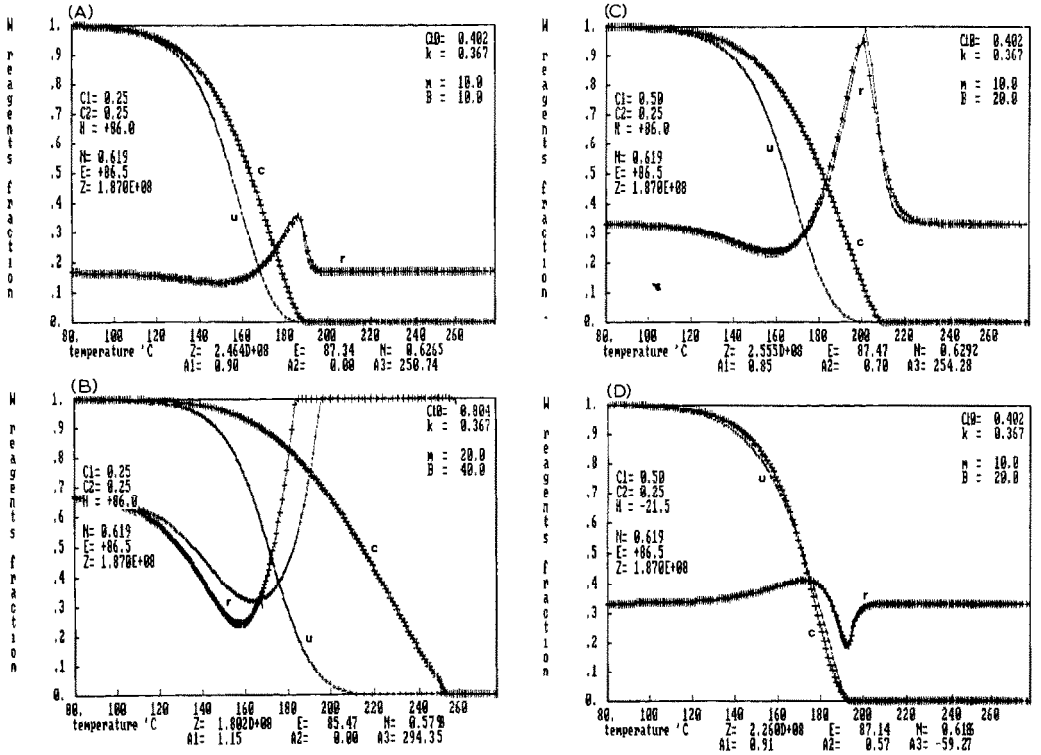

Fig. 2. Simulation: calculated W vs. T_p (c), W vs. T (u) and dT/dt vs. T (r) curves. W is $(m - m_f)/(m_i - m_f)$; T and T_p are temperatures in °C; time is in s. The values used to generate the curves are displayed in the figure, whilst the last rows show the kinetic parameters and mixed thermal coefficients as calculated from the simulated $W-T_p$ curve. The r curves are reported at two iteration steps. A–D show different cases.

$a3$ are sufficient to describe the model. In Figs. 2C and 2D the $C1$ and H values were changed to show the behaviour of the model when a variation in the specific heat and/or an exothermic reaction occur.

The isothermal half-life times, i.e. the times required to obtain $W = 0.50$, were measured at 120 °C, 130 °C and 140 °C, after heating the sample at 50 °C min^{-1} up to the chosen temperature. The ranges, obtained with three determinations at each temperature, are listed in Table 3 with the values

TABLE 3

Calcium oxalate dehydration. Determined ranges of isothermal half-life times (in s) at several temperatures (in °C), calculated values and errors introduced by temperature unaccuracy

Temperature	Found	Calculated	Error
120	1130–1160	1010	136
130	495– 530	524	67
140	270– 290	280	34

calculated using eqn. (21) when using the above-reported kinetic parameters. In the same table, errors induced by the low accuracy of the sample temperature (owing to both calibration and reaction heat) are also reported. These errors are calculated by differentiation of eqn. (21)

$$\text{error}(t_{\frac{1}{2}}) = \left[E/(RT^2)\right] t_{\frac{1}{2}} \text{ error}(T) \tag{24}$$

with error(T) = 2° C.

An attempt was made to reduce the contribution of the reaction heat to error(T) by sample dilution with aluminium oxide [17]. Unfortunately the measurement of half-life times was not improved, probably owing to the influence of the evolved gas diffusion through the diluent.

DISCUSSION

With respect to the theoretical model, the mixed thermal coefficient $a2$ needed to be set to zero, while $a1$ remained independent of the sample mass. Within experimental error, the model is not sensitive to the low contribution of the sample specific heat variation during reaction, as it could be when applied to calculated data (see Figs. 2C and 2D) where on the other hand the accuracy of $a2$ determination is not so high. On the contrary, the reason for the independence of $a1$ with respect to mass is probably not the assumption that $C_{t0} = 0$. Instead, the ratio C_{t0}/m_i could be considered to be a constant, assuming that just the portion of the holder in contact with the sample, and so proportional to the sample mass, is really the heat capacity C_{t0} of the holder having the same temperature as the sample ($C_{t0}/m_i = C_o m_i/m_i = C_o$, heat capacity per unit sample mass); the rest of the holder would follow the programmed temperature T_p and k would mainly represent the coefficient of heat transfer from the holder to the sample and to the portion of the holder being in contact with it. Figs. 2A and 2B show the reconstruction procedure of two TG curves, representing the calcium oxalate dehydration, by using the kinetic parameters and thermal coefficients found. The agreement between the source parameters (displayed in the Figure) and those obtained using the iterative procedure from W–T_p curves (lower lines) is satisfactory. 2C and 2D shows the same when a change in the specific heat or an exothermic reaction take place.

Figs. 1A and 1B, as well as Table 2, show a very good predictive power of the proposed model, when considering a fairly wide range of operative conditions. This predictive power proves to be higher than that of other models previously discussed [4], especially when considering the agreement of the kinetic parameters, determined from dynamic measurements (TG), with the isothermal half-lives. Is this a solution of the highlighted dichotomy [14]? It could be so, within the limits of the model of course, and remembering that the kinetic parameters found, which represent the experimental

data well, are always 'true' in the sense previously reported [4]. Several Z,E,N triplets are in fact able to display a satisfactory predictive power, because of the low numerical stability of the model itself; it may thus be difficult to find 'correct' kinetic parameters.

The proposed method, however, allows the calculation of 'true' kinetic parameters from the available data, i.e. from just a single TG curve as well as from several curves recorded at different masses and heating rates. Of course, the higher the number of data, the higher the predictive power will be.

Moreover, eqn. (17) gives a method for calculating pseudo-DTA curves, i.e. $T_p - T$ vs. T_p, from TG curves, and this approach becomes very easy when $a1$ and $a2$ can be assumed to be zero, or when the contribution of the related terms can be neglected with respect to that representing the reaction heat. These pseudo-DTA curves will be different from those available using other equipment, owing to the different thermal geometry affecting, as discussed, the TG measurements also. Methods based on mixing DTA–DSC data with TG data, for example to improve enthalpy measurements [18], could thus be used with great care.

When dealing with the kinetic parameters and calorimetric results obtained several considerations can be made: (i) the apparent reaction order N is close to the $\frac{2}{3}$ value of a phase-boundary-controlled three-dimensional process [16]; (ii) the activation energy E lies in the range of literature data previously reported [4], whilst its predictive power can be evaluated when considering only the entire triplet Z,E,N; (iii) the enthalpy of reaction H is about 20% higher than that due to the evaporated water evolved, i.e. about 70 cal g^{-1} of oxalate around 100 °C (this accounts for an endothermic reaction also when considering only the water leaving the solid oxalate); (iv) the specific heat values are not very far from those evaluated using the Dulong–Petit law, i.e. molar heat estimated to be $3Rn$ for n-atomic molecular solids.

REFERENCES

1 J.B. Henderson and T.E. Wiecek, J. Compos. Mater., 21 (1987) 373.
2 E.J. Kansa, H.E. Perlee and R.F. Chaiken, Combust. Flame, 29 (1977) 311.
3 G. Várhegyi, Thermochim. Acta, 110 (1987) 95.
4 U. Biader Ceipidor, R. Bucci, V. Carunchio and A.D. Magrí, Thermochim. Acta, 158 (1990) 125.
5 Z. Quanqin, L. Jinxiang and Z. Dianguo, Thermochim. Acta, 135 (1988) 187.
6 M. Tutaş, M. Sağlam, M. Yüksel and Ç. Güler, Thermochim. Acta, 111 (1987) 121.
7 E. Urbanovici and E. Segal, Thermochim. Acta, 118 (1987) 65.
8 J.P. Elder, Thermochim. Acta, 95 (1985) 41.
9 J.A. Cusido, J. Puigdomenech and C. Bonet, Thermochim. Acta, 114 (1987) 201.
10 L. Reich, L.Z. Pollara and S.S. Stivala, Thermochim. Acta, 111 (1987) 379.
11 El-H.M. Diefallah, S.N. Basahl, A.Y. Obajd and R.H. Abu-Eittah, Thermochim. Acta, 111 (1987) 49.

12 A. Romero Salvador and E. García Calvo, Thermochim. Acta, 107 (1986) 283.
13 L. Reich and S.S. Stivala, Thermochim. Acta, 124 (1988) 139.
14 P.D. Garn, Thermochim. Acta, 135 (1988) 71.
15 D. Dollimore, Thermochim. Acta, 117 (1987) 331.
16 J. Šesták, Thermochim. Acta, 3 (1971) 1.
17 W.W. Wendlandt, Thermal Analysis, Wiley, New York, 3rd edn., 1986.
18 J.B. Henderson, J.A. Wiebelt, M.R. Tant and G.R. Moore, Thermochim. Acta, 57 (1982) 161.